DOI 10.5162/Ultrasonic2025/C9-a4

Exploring the Potential of Plasma Microhollow Cathode Transducers for Air-Coupled Ultrasonic Non-Destructive Testing

Dmitry Solodov[1], *Narges Nazari*[1], *Mate Gaal*[1], *and Holger Kersten*[2]
[1] *Bundesanstalt für Materialforschung und -prüfung (BAM)*
[2] *Christian-Albrechts-Universität zu Kiel (CAU)*
dmitry.solodov@bam.de

Abstract: This study examines the feasibility of using Microhollow Cathode (MHC) plasma transducers as contactless, broadband sources for air-coupled ultrasonic nondestructive testing (NDT). To improve the detection of small or weakly bonded defects, the approach integrates Local Defect Resonance (LDR), which amplifies flaw responses at their natural vibrational frequencies.

Keywords: Microhollow cathodes, NDT, LDR, Air-coupled ultrasound

Introduction

Ultrasonic nondestructive testing (NDT) is crucial for assessing material and structural integrity without compromising functionality. It is extensively used in aerospace, civil engineering, and manufacturing, where early defect detection ensures safety and durability. Conventional ultrasonic methods rely on piezoelectric transducers requiring direct contact and coupling media such as water or gel, limiting their application on delicate, rough, or complex surfaces.

To address these limitations, air-coupled ultrasonic techniques have gained interest. Notably, Microhollow Cathode (MHC) plasma transducers offer a novel, compact alternative by generating pressure waves via pulsed plasma discharges in air. This enables high-frequency, broadband excitation without contact or coupling layers [1], making MHCs ideal for inspecting advanced materials like composites, polymers, and 3D-printed structures that are incompatible with traditional methods.

Concurrently, nonlinear ultrasonic techniques have enhanced sensitivity to subtle flaws. Local Defect Resonance (LDR) leverages defects natural vibrational frequencies, producing localized amplified responses detectable with high spatial resolution [2]. This frequency-selective approach improves detection of small defects often missed by conventional reflection-based methods.

This paper presents the integration of MHC plasma transducers and LDR into a fully air-coupled ultrasonic inspection system. Utilizing the broadband MHC emission and LDRs frequency sensitivity, the approach aims to improve flaw detectability while preserving non-contact benefits. The concept is validated through simulations and experimental results on polymer samples measured with laser Doppler vibrometry.

Micro-Hollow Cathode Plasma Transducers

Micro-Hollow Cathode (MHC) plasma transducers operate by initiating a pulsed discharge in a confined gas volume between closely spaced electrodes, typically separated by a gap. When a high-voltage pulse is applied across the gap, a stable glow discharge forms within the microcavity, rapidly heating the surrounding gas and producing ion movement that drives ionic wind, both of which contribute to localized pressure waves. This localized heating results in sudden thermal expansion, generating an acoustic pressure wave that propagates through air as a broadband ultrasonic pulse [1].

The electrical breakdown mechanism responsible for plasma formation is governed by Paschen's Law, which relates the breakdown voltage V_{BD} to the product of the gas pressure p and the gap distance d, i.e., $V_{\text{BD}} = f(pd)$. This empirical relationship assumes a uniform electric field between parallel-plate electrodes and does not explicitly account for electrode geometry.

A commonly used form of Paschen's Law is given by:

$$V_{\text{BD}} = \frac{B \cdot p \cdot d}{\ln(A \cdot p \cdot d) - \ln\left[\ln\left(1 + \frac{1}{\gamma_{\text{se}}}\right)\right]}, \qquad (1)$$

where A and B are gas-specific empirical constants, and γ_{se} is the secondary electron emission coefficient. While originally derived for idealized parallel-plate configurations, this expression provides useful insight into breakdown behavior in a variety of geometries. Micro hollow cathode (MHC) designs typically operate near the Paschen minimum, enabling stable discharge at relatively low voltages [3].

The discharge current within the cavity follows spatial patterns governed by the Helmholtz equation:

$$\nabla^2 j + k^2 j = 0, \tag{2}$$

leading to self-organized current density distributions that resemble acoustic mode shapes. The combined effects of thermal expansion and ionic wind contribute to acoustic emission. The ion velocity, which influences the strength of the acoustic wave, scales with discharge parameters [4] as

$$v_{\mathrm{ion}} \propto A\sqrt{\frac{\varepsilon_0}{\rho_0}} \cdot \frac{U_{\mathrm{HV}}}{d_g}, \tag{3}$$

where ε_0 is the vacuum permittivity, ρ_0 is the gas density, U_{HV} is the applied voltage, and d_g is the gap size.

Concept of Local Defect Resonance (LDR)

Local Defect Resonance (LDR) enhances ultrasonic flaw detection by targeting the natural vibrational frequencies of structural defects. These frequencies emerge due to local variations in stiffness and mass that arise from discontinuities such as voids, delaminations, or inclusions. When the structure is excited near one of these frequencies, the defect responds with significantly amplified, localized vibrations that can be detected remotely [5].

For instance, a cavity embedded in an elastic medium introduces a region of reduced stiffness, causing it to respond more dynamically to external excitation. Planar defects such as delaminations or disk-like cracks exhibit even greater changes in vibrational behavior due to their asymmetry and size. This resonance-based response provides a clear acoustic signature that enhances detectability, especially in composite or layered structures where traditional amplitude-based reflection techniques may fail.

The advantage of LDR lies in its frequency-selective sensitivity. By focusing on the resonant behavior of defects, it offers high contrast between defective and intact regions, improving localization and reducing false positives.

Analytical Modeling of Local Defect Resonance Frequency

To predict the resonance behavior of defects, analytical models based on classical plate theory are employed. A flat-bottom hole (FBH), commonly used as a model defect, is approximated as a circular, clamped thin plate. The natural frequency of this plate-like region can be expressed as:

$$f_{\mathrm{LDR}} = \frac{1}{2\pi}\sqrt{\frac{K_{\mathrm{eff}}}{m_{\mathrm{eff}}}}, \tag{4}$$

where K_{eff} and m_{eff} are the effective stiffness and mass of the defect region. Under idealized conditions, this can be further simplified to:

$$f_{\mathrm{LDR}} = \frac{\alpha}{2\pi}\frac{h}{R^2}\sqrt{\frac{E}{\rho(1-\nu^2)}}, \tag{5}$$

where h is the thickness of the plate, R its radius, E is Young's modulus, ρ the density, ν Poisson's ratio, and α a dimensionless parameter dependent on the boundary conditions [6].

The value of α varies depending on how the edges of the defect are constrained. Clamped edges yield higher frequencies and larger α, while simply supported or free boundaries reduce stiffness and lower the resonant frequency. Real defects seldom conform exactly to those predicted under idealized conditions of a homogeneous, isotropic material. While classical plate theory provides analytical estimates of resonant behavior based on simplified assumptions [7], accurate determination of the resonance parameter α often necessitates numerical modeling or empirical calibration to account for material anisotropy, geometric complexity, and boundary effects.

Despite their simplifications, these models offer valuable insights and enable pre-selection of excitation frequencies for LDR testing. They do, however, neglect damping, material anisotropy, and interaction with surrounding structures, all of which can affect the actual vibrational response. Therefore, analytical predictions are best used in conjunction with experimental or numerical methods.

Conceptual Framework for the Hybrid Technique

The integration of MHC plasma transducers with LDR forms a hybrid ultrasonic inspection method that combines the strengths of both technologies. MHC devices serve as compact, contactless, and broadband acoustic sources capable of exciting a wide range of frequencies. When these frequencies overlap with the natural resonance of a defect, the LDR mechanisms amplify the local response.

This synergy enables air-coupled excitation and the detection of defect-specific vibrations without the need for mechanical coupling, physical contact, or frequency tuning. A single broadband MHC pulse can stimulate multiple vibration modes within the test sample. If a defect resonance lies within the excitation spectrum, it will respond with a measurable increase in vibration amplitude, detectable using non-

contact sensors like laser Doppler vibrometers or air microphones.
By combining MHCs efficient broadband generation with the frequency-selective sensitivity of LDR, the system offers enhanced detection capabilities for small, subsurface, or weakly bonded defects. It is especially advantageous for inspecting composites or 3D-printed parts where traditional contact-based methods may be impractical.

Results

Three MHC plasma transducers with different geometrical configurations were employed in this study, differing in hollow diameter and electrode gap. For each configuration, the approximate high-voltage level required to ignite the plasma was determined experimentally. An overview of the geometries and corresponding ignition voltages is provided in Tab. 1.

Tab. 1: Geometrical configuration and ignition voltage of the three MHC plasma transducers.

hollow diameter (mm)	electrode gap (mm)	ignition voltage (kV)
1.0	1.6	~4.2
0.5	1.6	~7.5–9.0
0.5	1.0	~4.2

To characterize the acoustic behavior of the MHC-based transducers, a thin membrane was used as the target object, featuring a mass per unit area of 0.0163 $\frac{\mathrm{kg}}{\mathrm{m}^2}$. Plasma-induced pressure waves generated by the MHCs excited mechanical vibrations in the membrane, which were measured using laser Doppler vibrometry (LDV). Surface velocity measurements of the membrane were recorded with a Polytec OFV-505 sensor head combined with an OFV-5000 controller. The schematic measurement setup is shown in Fig. 1.

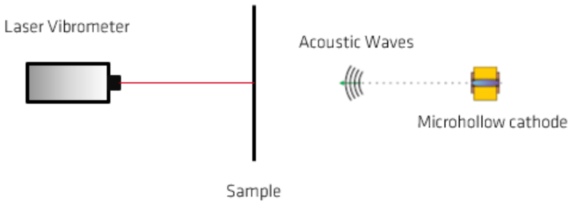

Fig. 1: Schematic setup for LDV-based characterization of MHC transducers.

Fig. 2 presents the membrane velocity signals for one representative MHC transducer. The plot consists of the time-domain response (top) and the corresponding frequency spectrum (bottom). The time-domain plot shows the velocity response of the membrane in $\frac{\mu\mathrm{m}}{\mathrm{s}}$ over time in milliseconds (ms), while the frequency spectrum illustrates the membrane velocity in $\frac{\mu\mathrm{m}}{\mathrm{s}}$ as a function of frequency in kilohertz (kHz). The distance between the membrane and the MHC transducer was 40 mm.

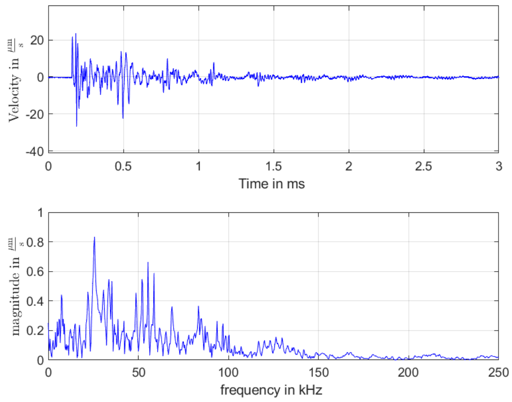

Fig. 2: Membrane response for one representative MHC transducers (1 mm hollow diameter 1.6 mm electrode gap) at 40 mm distance between membrane and transducer.

All transducers demonstrate broadband excitation with spectral content up to approximately 150 kHz.

This section presents an experimental study of a PMMA (polymethyl methacrylate) sample exhibiting a local defect resonance (LDR) near 7.6 kHz. This sample was selected due to its clear resonance behavior observed during preliminary tests.

The study aimed to identify and validate the resonance characteristics of two flat-bottom holes (FBHs) in the PMMA plate measuring $217\,\mathrm{mm} \times 30\,\mathrm{mm} \times 4\,\mathrm{mm}$. Each FBH had a diameter of $20\,\mathrm{mm}$ and a depth of about $3.6\,\mathrm{mm}$. The local defect resonance around 7.6 kHz was the focus.

A MHC transducer with a $1.6\,\mathrm{mm}$ electrode gap and $1\,\mathrm{mm}$ hollow diameter served as the excitation source. To avoid thermal overload during scans longer than five minutes, a transducer with reduced DC power consumption was used.

Initial vibrational responses of both FBHs were recorded using a 1D LDV following the setup shown in Fig. 1. Subsequent 3D scanning vibrometer measurements confirmed these findings. Frequency-domain analysis allowed comparison of resonance frequencies and evaluation of measurement consistency.

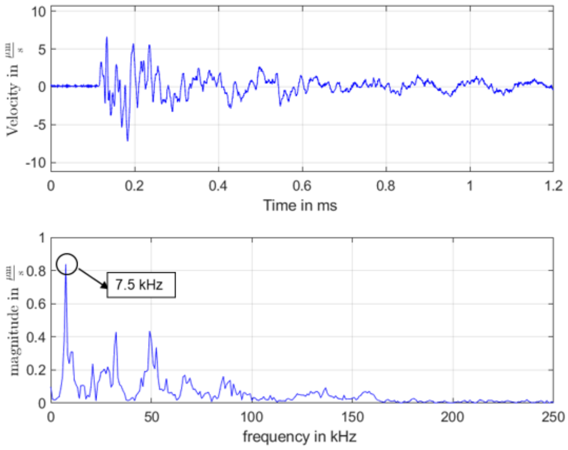

Fig. 3: PMMA sample (7.5 kHz), measurement with 1D laser doppler vibrometer

In both cases, a resonance frequency of 7.5 kHz was identified (see Fig. 3). This result was consistent across the two defects, indicating a reliable and reproducible detection of the LDR.

In order to verify the measurements obtained with the 1D LDV, additional scans were performed using a 3D scanning laser vibrometer. The resonance frequency of one FBH recorded from this method is shown in Fig. 4.

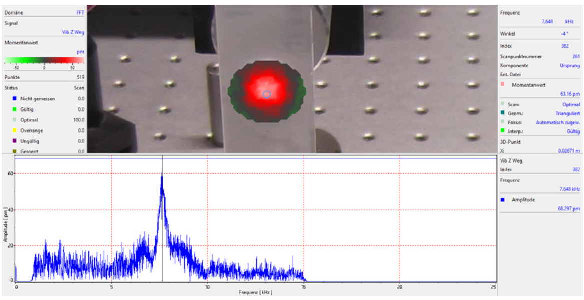
Domäne FFT
Signal Vib Z Weg
Momentanwert pm
Punkte 519
Status Scan
🟦 Nicht gemessen 0.0
🟩 Gültig 0.0
🟩 Optimal 100.0
🟨 Overrange 0.0
🟪 Ungültig 0.0
🟫 Gesperrt 0.0

Frequenz 7.648 kHz
Winkel -4 °
Index 382
Scanpunktnummer 261
Komponente Ursprung
Ent. Datei
Momentanwert 63.16 pm
Scan: Optimal
Geom.: Trianguliert
Fokus: Automatisch zugew.
Interp.: Gültig
3D-Punkt
X: 0.02671 m

Vib Z Weg
Index 382
Frequenz 7.648 kHz
🟦 Amplitude 68.297 pm

Fig. 4: PMMA sample, first FBH, LDR at 7.648 kHz (3D scanning vibrometer)

A resonance frequency of 7.648 kHz was detected at the first FBH, while the second FBH exhibited a resonance at 7.703 kHz.

Compared to the 1D LDV result (7.5 kHz for both FBHs), the relative deviation is 1.97 % for the first FBH and 2.71 % for the second FBH. These differences are within an acceptable range and confirm the accuracy of the initial 1D LDV measurements. Thus, the 3D vibrometer measurements serve as a supporting validation of the LDR frequency identified using the 1D system.

Conclusions

Experiments on PMMA samples with flat-bottom holes confirmed resonance frequencies near 7.6 kHz using both 1D and 3D laser Doppler vibrometry, closely aligning with analytical predictions. This validates the hybrid method's ability to reliably identify localized defects.

The synergy of MHCs broadband excitation and LDRs frequency-selective sensitivity improves defect detectability and spatial resolution, offering advantages for materials and geometries challenging for conventional contact-based ultrasonics.

Future work will extend this approach to diverse defect types and materials and optimize MHC transducer design for enhanced acoustic output and spectral control.

References

[1] I. Solodov, J. Bai, and G. Busse, Resonant ultrasound spectroscopy of defects: Case study of flat-bottomed holes, *Journal of Applied Physics*, vol. 113, no. 22, p. 223512, 2013. doi: 10.1063/1.4810926.

[2] W. Adebahr, I. Solodov, M. Rahammer, N. Gulnizkij, and M. Kreutzbruck, Local defect resonance for sensitive non-destructive testing, *AIP Conference Proceedings*, vol. 1706, no. 1, p. 050005, 2016. doi: 10.1063/1.4940504.

[3] M. S. Benilov, Comment on Self-organization in cathode boundary layer discharges in xenon and Self-organization in cathode boundary layer microdischarges, *Plasma Sources Science and Technology*, vol. 16, no. 2, p. 422, 2007. doi: 10.1088/0963-0252/16/2/N01.

[4] D. Kotschate, M. Gaal, and H. Kersten, Acoustic emission by self-organising effects of micro-hollow cathode discharges, *Applied Physics Letters*, vol. 112, no. 15, p. 154102, 2018. doi: 10.1063/1.5024459.

[5] I. Solodov, Resonant Acoustic Nonlinearity of Defects for Highly-Efficient Nonlinear NDE, *Journal of Nondestructive Evaluation*, vol. 33, pp. 252–262, 2014. doi: 10.1007/s10921-014-0229-9.

[6] Y. Zhang, L. Liu, Y. Chen, and J. Ouyang, Characteristics of ionic wind in needle-to-ring corona discharge, *Journal of Electrostatics*, vol. 74, pp. 15–20, 2015. doi: 10.1016/j.elstat.2014.12.008.

[7] A. W. Leissa, *Vibration of Plates*, NASA SP-160, U.S. Government Printing Office, Washington, D.C., 1969.